Journal of Hazardous Materials 186 (2011) 1300–1307

Contents lists available at ScienceDirect

Journal of Hazardous Materials

journal homepage: www.elsevier.com/locate/jhazmat

Biodegradation pathways of chloroanilines by *Acinetobacter baylyi* strain GFJ2

Parnuch Hongsawat[a], Alisa S. Vangnai[b,c,*]

[a] International Postgraduate Program in Environmental Management, Graduate School, Chulalongkorn University, Bangkok 10330, Thailand
[b] National Center of Excellence for Environmental and Hazardous Waste Management (NCE-EHWM), Chulalongkorn University, Bangkok 10330, Thailand
[c] Department of Biochemistry, Faculty of Science, Chulalongkorn University, Bangkok 10330, Thailand

ARTICLE INFO

Article history:
Received 20 July 2010
Received in revised form
26 November 2010
Accepted 1 December 2010
Available online 8 December 2010

Keywords:
4-Chloroaniline
3,4-Dichloroaniline
Monohalogenated aniline
Biodegradation pathway
Acinetobacter baylyi
Bioremediation

ABSTRACT

The *Acinetobacter baylyi* strain GFJ2 was isolated from soil that was potentially contaminated with herbicides. It exhibited complete biodegradations of 4-chlroaniline (4CA) and 3,4-dichloroaniline (34DCA), a wide range of monohalogenated anilines (chloro-, bromo-, and fluoro-anilines) and other dichloroanilines. An in-depth investigation of the biodegradation pathway revealed that a dechlorination reaction may be involved in 34DCA biodegradation, which forms 4CA as the first intermediate. By detecting the transient intermediates and characterizing the relevant enzymes, this investigation is also the first to report that *A. baylyi* strain GFJ2 has two distinct 4CA degradation pathways that yield 4-chlorocatechol (4CC) and aniline as the first intermediate in each route, which are further metabolized through an *ortho*-cleavage pathway. Analysis of biodegradation kinetics analysis illustrated that *A. baylyi* GFJ2 utilized aniline and 4CC at significantly slower rates than it used 4CA, suggesting that the transformations of aniline and 4CC were probably the limiting steps during 4CA biodegradation. Our results suggest the potential application of *A. baylyi* strain GFJ2 in bioremediation and waste treatment, and the kinetic data provide the insights into the degradation mechanism, dynamics and possible limitations of the biodegradation which include substrate and product inhibitions.

1. Introduction

Chloroanilines (CAs) are a group of chlorinated aromatic amines which are originated from the biotransformation of herbicides, for example phenylcarbamate, phenylurea, or acylanilides [1]. In addition, they are widely used as intermediate compounds in the production of dyes, polyurethanes, pesticides, and pharmaceutical products. As a consequence of intensive applications in agriculture and industries, chloroanilines, especially 4-chloroaniline (4CA) and 3,4-dichloroaniline (34DCA), have been ubiquitous and accumulated in the environment including agricultural soil/water, industrial wastewater and sludge. Due to their toxicity and recalcitrant properties, they have been considered as the important environmental pollutants and are subject to legislative control by the environmental protection agency of United States and Europe [2]. To dissimilate the environmental contaminated aniline and chloroanilines, bioremediation has been noted as a primary treatment technique in which a detoxification process is depending on the microbial biodegradability. Since the resistance of microbial biodegradation and toxicity of chloroanilines mainly depend on the number and position of chlorine atoms on the aromatic ring, there are many more reports of aniline-degrading bacteria than those of monochloroaniline (MCA)- or dichloroaniline (DCA)-metabolizing bacteria, some of which strictly required aniline as an inducer for cometabolic biodegradation [3]. In addition, while there are a number of publications describing microbial degradation of MCAs and DCAs under aerobic conditions, there are only a few reports on bacteria able to effectively degrade both chemical types. *Pseudomonas diminuta* was first bacterium described for its capability of degrading 3CA, 4CA and 34DCA (up to 0.3 mM), but not aniline [4], while *Alcaligenes faecalis* was reported for its ability to convert 34DCA to 4,5-dichloropyrocatechol before further metabolized [5]. Since the presence of MCAs and DCAs contaminated in the environment generally appears as co-contaminants, therefore to improve the biological remediation, microorganism with biodegradability of both MCAs and DCAs is importantly required. Moreover, in-depth information of its biodegradation pathway as well as biodegradation kinetics is necessary in order to have thorough understanding of biotransformation process which will further lead to effective control of bioremediation system.

In the present study, we successfully isolated and characterized 4CA-degrading bacterium, *Acinetobacter baylyi* strain GFJ2, which has a broad range biodegradability towards various halogenated anilines. Investigation of biodegradation kinetics and

* Corresponding author at: Department of Biochemistry, Faculty of Science, Chulalongkorn University, Phayathai Street, Pratumwan District, Bangkok 10330, Thailand. Tel.: +66 2 218 5430; fax: +66 2 218 5418.
E-mail addresses: alisa.v@chula.ac.th, avangnai@yahoo.com (A.S. Vangnai).

0304-3894/$ – see front matter © 2010 Elsevier B.V. All rights reserved.
doi:10.1016/j.jhazmat.2010.12.002

biodegradation inhibition profiles were also carried out for single substrates and mixed substrates. Interestingly, transient intermediate detected during biodegradation of 34DCA suggested a novel reaction involving dechlorination of 34DCA, while those detected during 4CA degradation leaded us to propose that two different biodegradation pathways of 4CA are existed in *A. baylyi* strain GFJ2. These results not only illustrated in-depth information of biodegradation mechanism of 34DCA and 4CA in *A. baylyi* strain GFJ2, but its effective biodegradability also demonstrates its potential application for bioaugmentation in the bioremediation treatment of contaminated site.

2. Materials and methods

2.1. Chemicals and cultivation medium

4-Chloroaniline (4CA), 2,3-dichloroaniline (23DCA), 2,4-dichloroaniline (24DCA), 3,4-dichloroaniline (34DCA), and 3,5-dichloroaniline (35DCA) (99% purity) (Chem Service, USA) were dissolved in high quality methanol (Fisher Scientific, USA) prior to use. Aniline (Merck, Germany), 2-chloroaniline (2CA) and 3-chloroaniline (3CA) (99% purity) (Chem Service, USA) were used as liquid. The chemicals for cultivation medium were analytical grade from Scharlau Microbiology, Spain. The minimal medium (MM) (pH 7.0) was prepared according to Vangnai and Petchkroh [6]. When supplemented with yeast extract (0.1%, w/v), the medium was designated as MMY. The media were solidified with 15 g L^{-1} of agar for cell cultivation on a medium agar plate.

2.2. Isolation and identification of chloroaniline-degrading bacterium

Samples for bacterial isolation were collected from several sources including pristine soil, soil and surface water from agricultural areas with history use of herbicide and agricultural products exposed to herbicides and contaminated soil. The bacterial isolation was performed by plating soil suspension or liquid samples or placing a part of agricultural products directly on to an agar plate containing either MM or MMY containing 4CA or 34DCA or a combination of 4CA and 34DCA (0.2 mM each) and incubated in an incubator at 30 °C. Bacterial colonies formed on the plate were collected, repeatedly purified and then selected for further investigation. The CA-degrading bacteria was then identified by morphology, biochemical test and 16S rRNA sequence analysis according to Vangnai and Petchkroh [6]. Partial 16S rRNA gene sequence was aligned and compared with the sequences placed in Genbank using BLASTN.

2.3. Parameters affecting cell growth and 4CA biodegradation

The effects of nutrient component on bacterial growth and biodegradation of 4CA were examined. The isolate was grown in Luria–Bertani (LB) medium or MMY supplemented with one of the following carbon sources (1 g L^{-1}): glucose, glycerol; nitrogen source (1 mM): ammonium sulfate, sodium nitrate, urea; energy source (4 mM): succinate, citrate, pyruvate, each of which contained 4CA at 0.2 mM. Then, cells were incubated at 30 °C with shaking condition at 200 rpm. At the indicated time, cell turbidity was determined at 560 nm (DU800, Beckman Coulter, Inc., USA) and 4CA remained in the supernatant was determined using HPLC.

2.4. Biodegradation of aniline and halogenated anilines

All biodegradation experiments were carried out aerobically in 250-ml flasks at 30 °C with a constant shaking at 200 rpm. Each substrate, i.e. MCA, DCA, BA, and FA, was provided at the initial concentration of 0.2 mM (unless otherwise stated) to a 100-ml medium containing 1% (v/v) cell inoculum. Cell samples were interval collected at the time indicated. Bacterial growth was determined by measuring cell optical density at 560 nm. Disappearance of the test substrate was taken as an indicator of substrate utilization. Abiotic control was also carried out to account for the substrate dissimilation caused by other physical factor, e.g. photo-degradation, if any.

2.5. Preparation of cell-free extract and enzyme assays

Cells (100 ml) were harvested by centrifugation for 20 min at 11,000 × *g* at 4 °C, washed twice and suspended with 5 ml of 50 mM Tris–HCl buffer pH 7.8. Cells were disrupted using a French pressure cell (Thermo Electron Corporation, USA) twice at 12,000 psi. Cell debris was removed by centrifugation at 11,000 × *g* for 20 min at 4 °C. The cell-free supernatant was used immediately after the preparation for the activity assays of catechol 1,2-dioxygenase (C12O), chlorocatechol 1,2-dioxygenase (CC12O), catechol 2,3-dioxygenase (C23O) and chlorocatechol 2,3-dioxygenase (CC23O) according to Vangnai and Petchkroh [6].

2.6. Analytical methods

The biodegradation of aniline, chloroaniline and the accumulation of intermediate(s) were analyzed by a reverse phase high performance liquid chromatography (HPLC) equipped with a UV detector (240 nm). The separation was performed at 40 °C on C18 HPLC column (5 μm, 250 mm × 4.6 mm; Hyperclone, Phenomenex, USA) using acetronitrile: water mixture (70:30%, v) as the mobile phase at a flow rate of 1 ml min^{-1}. Qualitative and quantitative data were obtained by comparing the peak area of unknown peaks with those of the standard compounds with known concentration.

The GC/MS analysis of biodegradation intermediates were performed using a GC (Agilent 6890N, CA, USA) equipped with an inert mass selective detector (Agilent 5973, CA, USA). The analysis was carried out on a DB-5ms capillary column (0.25 mm × 30 m × 0.25 μm) with a spiltless mode using nitrogen as carrier gas at a flow rate of 1.5 ml min^{-1}. The intermediates were identified on the basis of mass spectra and retention time using the mass spectral library PEST.L [7].

Chloride determination was carried out using an ion chromatography (LC25 chromatography, DIONEX, IL, USA) equipped with an electrochemical detector (ED50, DIONEX, IL, USA) and an Ion Pac AS19 column (4 mm × 250 mm) using KOH solution (28 mM) as an eluent with a flow rate of 1.2 ml min^{-1} at 30 °C. The measurement was carried out with a 20-μl sample size and amount of chloride was quantitatively determined using a calibration curve of a chloride standard (NaCl in water, Merck, Darmstad, Germany).

2.7. Biodegradation kinetic analysis

Kinetics studies were carried out using resting cell culture. Overnight grown cells in the minimal medium supplemented with succinate (4 mM), ammonium sulfate (1 mM) and yeast extract (0.1%, w/v) (MMSAY) (100 ml) were harvested, concentrated to the final optical density of approximately 2.0 before each test substrate was added to the indicated concentration to start the biodegradation experiment. The substrate degradation rates were then calculated from a plot of the substrate concentration versus time. A single substrate kinetic test was carried out with at least four different substrate concentrations. Then, the kinetic parameters, k_{max} and K_s^{app} values, of each substrate were derived by a linear regression fitting of data points according a non-growth Michaelis–Menten model developed by Schmidt et al. [8], i.e. $-dS/dt = k_0 S/(K_s^{app} + S)$

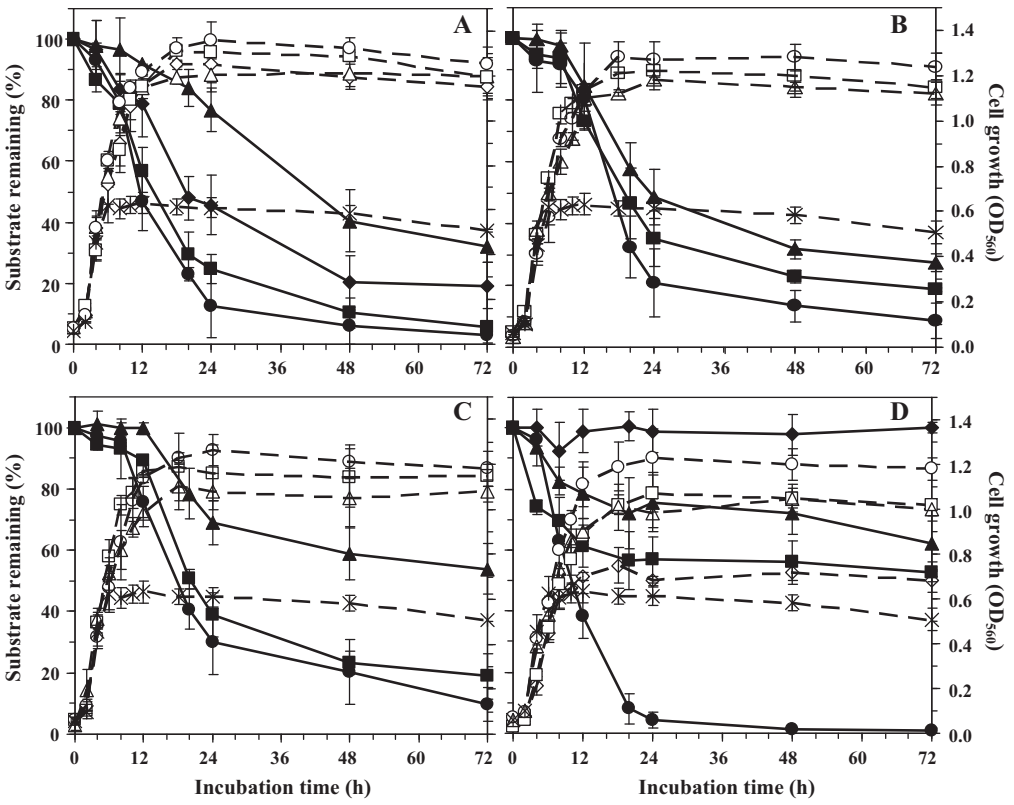

Fig. 1. Growth (opened symbol, dashed line) and biodegradation of aniline and halogenated aniline shown as the remaining substrate percentage (closed symbol, solid line) of *Acinetobacter baylyi* GFJ2. Cells were grown on the MMSAY medium supplemented with 0.2 mM of each substrate (symbol shown in order: growth, biodegradation). (A) Aniline and monochloroanilines: 2CA (△,▲), 3CA (□,■), 4CA (○,●), and aniline (◊,♦). (B) Bromoanilines: 2BA (△,▲), 3BA (□,■), 4BA (○,●). (C) Fluoroanilines: 2FA (△,▲), 3FA (□,■), 4FA (○,●). (D) Dichloroanilines: 23DCA (◊,♦), 24DCA (□,■), 34DCA (○,●), and 35DCA (△,▲). Cell growth on the MMSAY medium alone was shown as a control (*). Data are means of the results from at least four individual experiments. Error bars indicate standard errors.

under a condition in which $B_0 = B_{max}$, where B_0 is starting cell population density, B_{max} is maximum cell population density, and $k_0 = k_{max}B_0$. The inhibition kinetics study was carried out between a pair of substrate as indicated. The inhibition type and inhibition coefficients were derived according to a modified Cornish–Bowden relation [9]. Regression analysis was performed with the data analysis tool pack of Microsoft Excel® and the model equations were solved using GraphPad Prism 5 software (CA, USA).

3. Results and discussion

3.1. Isolation and characterization of strain GFJ2

Isolate GFJ2 was a gram negative, coccus-shaped bacterium. It was isolated from soil swapped from fruit peels and selectively isolated on a minimal medium agar containing 0.2 mM 4CA. Therefore, it was initially identified as a 4CA-degrading bacterium. Bacterial identification using a 16S rRNA sequence analysis revealed high similarities to the following strains: 97% similarity to rice-associated bacterium *A. baylyi* strain 3R22 (EF178435.1), 97% similarity to *A. baylyi* strain H8 (FJ009373), and 97% similarity to *A. soli* strain B1 (EU290155.1) (formerly *A. baylyi* strain B1) isolated from forest soil. Therefore, the bacterial isolate GFJ2 was designated as *A. baylyi* strain GFJ2. The partial 16S rDNA gene sequence analyzed using BLASTN program was submitted to the GenBank nucleotide sequence database (NCBI) with the accession number HQ611277.

Prior to further investigation, the influence of nutrients on growth and 4CA biodegradation was investigated. Because the yeast extract (0.1%, w/v) supplemented in the culture medium was strictly required to maintain growth and resulted in the 4CA biodegradation rate of 0.075 ± 0.002 μmole h^{-1} mg cell protein^{-1}, the effects of other nutrient components were evaluated in a minimal medium supplemented with yeast extract (MMY). *A. baylyi* GFJ2 grew well in each nutrient tested, but the 4CA utilization rates were different to some extents. Supplementation with glucose and glycerol prolonged biodegradation lag period for 4 h and reduced the 4CA biodegradation rate by 22% and 35%, respectively. This result agreed with the previous report that showed that glucose causes an approximately 10-h growth-lag period and represses the aniline utilization of *P. multivoran* An1 by 77–99% [10]. Supplementation with ammonium sulfate as a nitrogen source increased the 4CA biodegradation of *A. baylyi* GFJ2 by 16% while the addition of sodium nitrate and urea decreased the degradation rate by 10% and 40%, respectively. The addition of succinate, citrate and pyruvate as an energy source increased the biodegradation of 4CA by 15%, 6%, and 5%, respectively. These results are in contrast with the report showing that, in *P. multivoran* An1, pyruvate and succinate strongly repress cell activity to utilize aniline [10]. Moreover, supplementation of the MMY medium with both ammonium sulfate and succinate significantly enhanced the 4CA biodegradation rate of *A. baylyi* GFJ2 by 25 ± 2%.

Therefore, further investigations of the biodegradation of aniline and halogenated anilines were conducted using MMY supplemented with ammonium sulfate and succinate (MMSAY).

3.2. Biodegradation of aniline and halogenated anilines by A. baylyi GFJ2

The growth of *A. baylyi* GFJ2 was well supported by the MMSAY medium, and significantly enhanced when aniline or MCA was added (Fig. 1A). However, in the presence of the supplemented

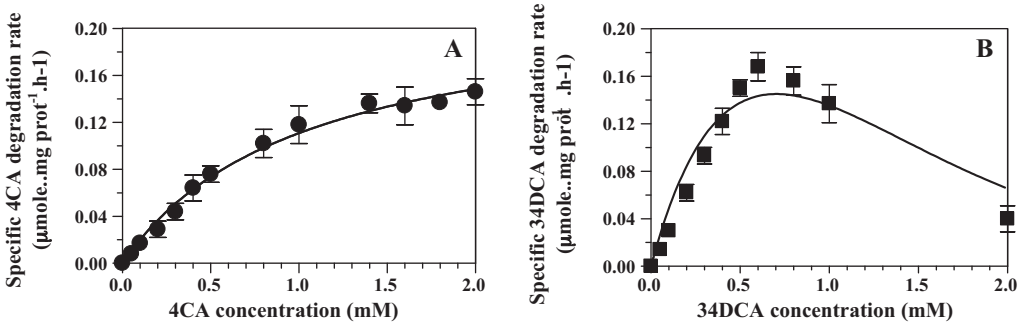

Fig. 2. Relationship between the specific biodegradation rate and the concentrations of 4-chloroaniline (●) and 3,4-dichloroaniline (■) (similar to v versus S curve) by *Acinetobacter baylyi* GFJ2. The data points were derived from substrate-depletion curve and fitted with Michaelis–Menten equation (A) and the modified Michaelis–Menten equation (i.e. Edwards model) (B) by the non-linear least-squares method.

nutrients, we could not conclude that *A. baylyi* GFJ2 utilized aniline or MCA as the sole sources of carbon and nitrogen for cell biomass production. Nevertheless, it was clearly shown that *A. baylyi* GFJ2 was capable of degrading them by the disappearance of the substrate and the liberation of chloride. *A. baylyi* GFJ2 degraded aniline and MCA at the following biodegradation rate (μmole h^{-1} mg cell $protein^{-1}$) and total biodegradations (expressed as % degradation): 4CA (0.087 ± 0.016; $97 \pm 3\%$) > 3CA (0.082 ± 0.014; $94 \pm 1\%$) > aniline (0.062 ± 0.002; $81 \pm 7\%$) > 2CA (0.022 ± 0.003; $68 \pm 5\%$) (Fig. 1A). After 24-h of the incubation, the stoichiometric liberation of chloride (i.e. 0.16 ± 0.03 mM) confirmed the relatively complete biodegradation of 4CA. Interestingly, while most of the previously reported MCA-degrading bacteria particularly required aniline as either a co-metabolic substrate or as an inducer [6,11], neither aniline nor any other inducer was required for *A. baylyi* GFJ2.

To assess the biodegradability range of *A. baylyi* GFJ2 on other monohalogenated anilines, a series of bromoanilines (BA) (Fig. 1B) and fluoroanilines (FA) was evaluated (Fig. 1C). Upon cell exposure to each of the BA and FA isomers, a biodegradation lag phase of approximately 12 h and a subsequent reasonable biodegradation rate were observed for each compound. This result indicated that an acclimatization process, such as an induction or a de-repression of enzymes or an adaptation to the toxic chemical, occurred and allowed the bacteria to cope with the toxicity of BA and FA before further degradation [12]. *A. baylyi* GFJ2 degraded 3BA, 3FA, 4BA, and 4FA at rates and total biodegradations similar to those of 3CA and 4CA, while it was able to degrade 2BA and 2FA with 2.6 and 2.2 times higher rates than that of 2CA, respectively. However, the higher biodegradation rate of 2FA did not reflect the total biodegradation as it only reached $46 \pm 8\%$ biodegradation after 5 days of incubation (Fig. 1C).

Previous studies have stated that the microbial transformation of substituted aromatic compounds depends on the number and position of the substituted atom in the molecule. For instance, the chloroaniline utilization rate in *P. multivorans* An1 was decreased in the order of 3CA > 2CA > 4CA and was insignificant for 34DCA [13]. In contrast, 3CA and 4CA were the preferred substrates of *A. baylyi* GFJ2 and had a rate 4 times faster than that of 2CA. Aside from the substituent position, it has been suggested that the steric properties of substituted group likely control the biodegradation rate [14]. It has been demonstrated that a small substituent with a low value of van der Waals radius (such as hydrogen or fluorine) allows a faster aniline turnover, whereas a bulky substituent (such as chlorine, bromine, or iodine) precludes a rapid metabolism. However, such an effect was not apparent in *A. baylyi* GFJ2. These results show that *A. baylyi* GFJ2 has broad substrate specificity towards halogenated anilines, especially 4CA and 3CA.

Several microorganisms have been reported to have limited capabilities to degrade either MCA [6,15] or DCA [3,16]. However, to be useful for further applications in bioremediation, broad range biodegradability is a preferred cell characteristic. Interestingly, *A. baylyi* GFJ2 was able to completely degrade 34DCA at a relatively high rate (0.116 ± 0.010 μmole h^{-1} mg cell $protein^{-1}$) and with a stoichiometric release of chloride (0.19 ± 0.03 mM). It moderately degraded 24DCA and 35DCA at rates that were 2.6 and 3.5 times slower and reached totals of $47 \pm 3\%$ and $38 \pm 9\%$, respectively, while it could not degrade 23DCA (Fig. 1D). The ability of *A. baylyi* GFJ2 to degrade 34DCA was observed even in the absence of any stimulating chemicals or co-substrate which is contrary to the reports stating that a specific inducer, such as propionanilide [17], aniline [16], or 4CA [18] is strictly required.

3.3. 4CA- and 34DCA biodegradation kinetics and intermediates

Whole-cell biodegradation kinetic was investigated to elucidate the biodegradation characteristics of *A. baylyi* GFJ2. It should be noted that these experiments were performed with whole cells, therefore it cannot be ruled out that the substrate transport limitations and other cell dynamic processes may influence the kinetic characteristics observed [19]. Two best-known kinetic models are Monod equation and Michaelis–Menten equation. Although their equations are somewhat similar, their intrinsic significances are different. The kinetics of substrate mineralization are theoretically expressed as the relationship between growth rate and substrate concentration, as described by Monod [20,21]. The biodegradation characteristic of the substrate is likely to follow a saturating kinetics described by a modified Michaelis–Menten relationship, where the initial substrate concentration (S_0) to biomass (X_0) ratio is of important concern [8]. Generally, the kinetics assay is initially conducted at high value of S_0/X_0 which allows several cell divisions as well as significant physiological and biochemical changes in the cells. However, in this study, the kinetics assays were performed using high density cells (resting cells) and no significant increase in cell numbers was observed during the test ($B_0 \cong B_{max}$, where B is cell population density) [8]. Under the conditions recommended for the batch biodegradation test, changes in both the biochemical reactions and the physiological states of cells were minimal [22]. Consequently, the kinetics observed under such conditions represent an immediate response that described the cell's biodegradation capability for the target substrate [22,23]. The biodegradation kinetic profile of 4CA by *A. baylyi* GFJ2 followed the saturation kinetics of a Michaelis–Menten-like relationship (Fig. 2A). In contrast, the 34DCA biodegradation rate was decreased at high substrate concentrations and the kinetic profile fitted with the Edwards model well (Fig. 2B), suggesting that a substrate inhibition was occurred [24]. The kinetic parameters derived by

Table 1
Apparent kinetic parameters of the biodegradation of chloroanilines and the related compounds by *Acinetobacter baylyi* GFJ2.

Substrate	Inhibitor	K_s^{app} (mM)	k_{max} (μmole h^{-1} mg protein^{-1})	k_{max}/K_s^{app} ($\times 10^{-3}$)	K_i^{app} (mM)	K_I^{app} (mM)	Inhibition type
34DCA	–	0.70 ± 0.02	0.36 ± 0.02	0.51 ± 0.02	0.73 ± 0.03[a]	–	–
4CA	–	0.79 ± 0.12	0.17 ± 0.01	0.22 ± 0.02	–	–	–
Aniline	–	2.57 ± 0.10	0.09 ± 0.02	0.04 ± 0.01	–	–	–
4CC	–	0.33 ± 0.01	0.05 ± 0.01	0.15 ± 0.03	–	–	–
34DCA	4CA	–	–		0.105 ± 0.020	0.120 ± 0.015	Mixed
4CA	Aniline	–	–		0.64 ± 0.060	–	Competitive
4CA	4CC	–	–		–	0.115 ± 0.030	Uncompetitive

K_s^{app}, the apparent half-saturation coefficient; k_{max}, the specific biodegradation rate; K_i^{app}, the apparent inhibition coefficient, i.e. an equilibrium constant where an inhibitor (I) binds to a free enzyme (E) to form an enzyme–inhibitor complex (E–I) (competitive); K_I^{app}, the apparent inhibition coefficient, i.e. an equilibrium constant where an inhibitor (I) binds to an enzyme–substrate complex (ES) to form an enzyme–substrate–inhibitor complex (ESI) (uncompetitive).

[a] Substrate inhibitory effect.

a nonlinear least-squares method and linear regressions using a double-reciprocal plot were similar (Table 1 and Fig. 5A and B). *A. baylyi* GFJ2 exhibited K_s^{app} for both 4CA and 34DCA within the similar range, but the k_{max} values were markedly different. Accordingly, the values of k_{max}/K_s^{app} that represent substrate uptake competition in a single bacterial strain indicated that *A. baylyi* GFJ2 prefers to utilize 34DCA twice as much as 4CA (Table 1).

3.4. Detection of biodegradation intermediates and the proposed 4CA and 34DCA biodegradation pathways in A. baylyi GFJ2

During 34DCA biodegradation at a high concentration, HPLC analysis revealed a transient accumulation of the compound with a peak retention time similar to that of 4CA (3.51 min). A spiking method with a 4CA reference standard and GC–MS analysis with a comparison of the fragment ions with authentic chemical in the positive ion mode indicated that the 4CA at *m*/*z* 127 [MH^+] was indeed the intermediate of 34DCA biodegradation (Fig. 3A). 4CA formation was detected only under aerobic condition (data not shown) and strictly in the presence of cells. 4CA formation was not detected in the abiotic control, implying that 34DCA degradation in *A. baylyi* GFJ2 initially proceeds through an enzyme-catalyzed dehalogenation [25]. Microbial dehalogenation can occur through several reaction types, such as hydrolytic dehalogenation, dehydrohalogenation, and monooxygenation [25]. However, in this case, the transformation of 34DCA into 4CA suggested that a reductive dehalogenation under aerobic condition might be involved. Although aerobic bacteria do not typically conduct reductive dehalogenation reaction, such reactions are not unprecedented. For example, the reductive dehalogenation of tetrachlorohydroquinone occurs under aerobic condition catalyzed by glutathione transferase in *Sphingobium chlorophenolicum* [26]. The mechanism and the enzyme involved in aerobic dehalogenation in *A. baylyi* GFJ2 have yet to be investigated. Nevertheless, the finding that 4CA is the intermediate in the 34DCA biodegradation pathway is novel and is in contrast with previous reports. The widely known 34DCA biodegradation pathway generally follows that of *P. putida* where 34DCA is transformed by a dioxygenase, forms 4,5-dichlorocatechol, and is subsequently mineralized [17]. Another pathway was reported in *P. fluorescens* 26-K, where 3,4-dichloroacetanilide (formed by acylation) and 3,3′,4,4′-tetrachloroazoxybenzene (formed by polymerization) were detected as the intermediates [16].

Further investigation of 4CA biodegradation at a high concentration also revealed the transient accumulation of the corresponding intermediates. A spiking method with the reference standard compound and GC–MS analysis found that 4CA was converted into two intermediates, aniline (HPLC 3.16 min and *m*/*z* 93 [MH^+]) and 4CC (HPLC 2.96 min and *m*/*z* 172 [MH^+]) (Fig. 3B). The result suggests that two degradation pathways exist in *A. baylyi* GFJ2. The consistent detection of 4CC agrees with the previous reports stating that 4CA biodegradation is initially catalyzed through a dioxygenase that forms 4CC as the intermediate [1,15]. The intermediate then proceeds into a ring cleavage reaction through either *ortho*-cleavage or *meta*-cleavage. However, the discovery that aniline is one of the transient metabolites was intriguing because it implied that aniline is formed from the cleavage of the 4CA chlorine atom probably by an enzyme-catalyzed dechlorination. These data represent the first evidence that 4CA can potentially be metabolized through two distinct biodegradation pathways: the initial action of dioxygenation (presumably chloroaniline dioxygenase) that form 4CC and the dechlorination that form aniline. It should be noted that the detection of the intermediates was successful only when

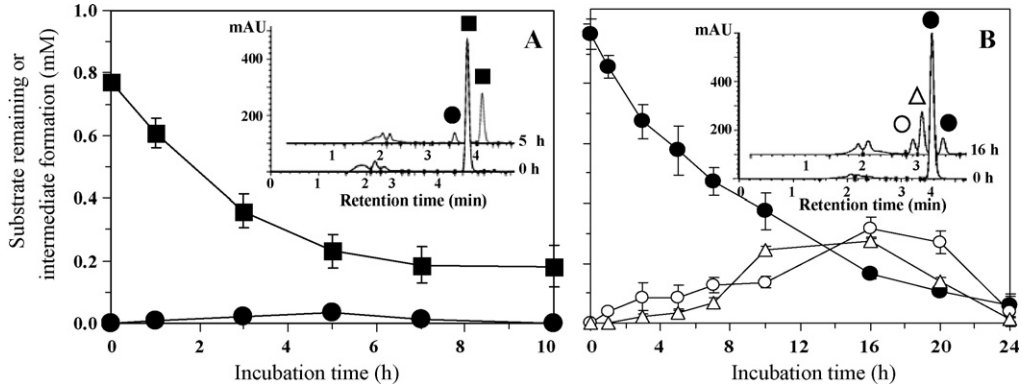

Fig. 3. The formation of the intermediates during the biodegradation of 34DCA (A) and 4CA (B) in *Acinetobacter baylyi* GFJ2. In (A), during 34DCA biodegradation (■), 4CA (●) of which the peak was at 3.51 min was formed. In (B), during 4CA biodegradation (●), the formation of 4CC (○) (2.96 min), and aniline (△) (3.16 min) were observed. The inlets show the overlay of the corresponding HPLC peaks at the indicating incubation time. The inlet *y*-axis represents the HPLC signal intensity expressed by a milli-HPLC arbitrary unit (mAU). Data are means of the results from three individual experiments. Error bars indicate standard errors.

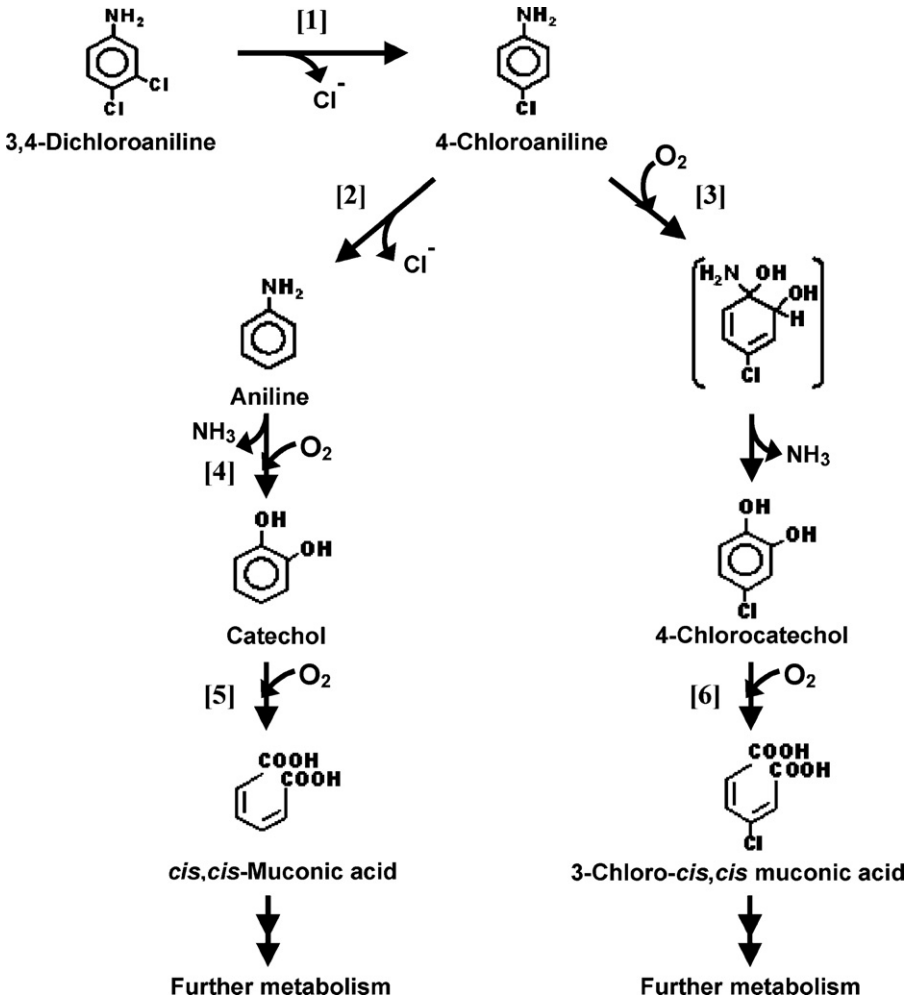

Fig. 4. The proposed biodegradation pathway for 3,4-dichloroaniline and 4-chloroaniline in *Acinetobacter baylyi* GFJ2. The reaction or enzyme activity are denoted as follows: [1], dechlorination; [2], dechlorination; [3], dioxygenation tentatively by chloroaniline dioxygenase; [4], dioxygenation tentatively by aniline dioxygenase; [5], catechol 1,2-dioxygenase; [6], chlorocatechol 1,2-dioxygenase.

the experiment was conducted with the resting cell suspension, and not cells under the growth conditions that rapidly metabolized the metabolic intermediates.

3.5. Characterization of the enzyme activities involved in 4CA- and 34DCA biodegradations

To confirm the existence of two distinct 4CA biodegradation pathways, the activities of aniline dioxygenase (Fig. 4, reaction [4]) and chloroaniline dioxygenase (Fig. 4, reaction [3]) were initially examined in a cell-free extract of *A. baylyi* GFJ2 pre-grown with 4CA. However, the determination of both enzyme activities was unsuccessful, probably due to the low stabilities of the enzymes in the cell-free extract. Therefore, the activities of the enzymes that potentially exist in the downstream degradation pathways, i.e. C12DO or C23DO (Fig. 4, reaction [5]), CC12DO or CC23DO (Fig. 4, reaction [6]), were examined in the cell-free extract. The determination of these enzyme activities was conducted not only to confirm the presence of two distinct pathways for 4CA biodegradation, but also to elucidate whether the degradation proceeded *via ortho*- or *meta*-cleavage pathway. The results (Table 2) clearly show that *A. baylyi* GFJ2 does not use a *meta*-cleavage pathway to degrade 4CA and 34DCA because C23DO and CC23DO activities were not detected. Low levels of C12DO and CC12DO activities were detected from non-induced cells, suggesting that both enzymes were partly constitutive. Nevertheless, the enzyme activities were substantially induced when each specific substrate was provided. The activity of C12DO was noticeably enhanced when the cells were grown with either aniline or catechol indicating that aniline and catechol were utilized through an *ortho*-cleavage pathway. However, the activity of CC12DO was induced in the presence of a chlorinated aromatic compound (i.e. 4CC), indicating that a modified *ortho*-cleavage pathway was responsible for 4CC degradation. When the cells were grown with the chlorinated anilines (i.e. 34DCA or 4CA), significant activities of both C12DO and CC12DO were detected, which indicated that the *ortho*-cleavage and the modified *ortho*-cleavage pathways were induced in response to cell exposure to 34DCA and 4CA. These results consistently supported that 4CA was degraded through two distinct biodegradation pathways. Previous reports have shown that the degradation of chloroanilines typically occurs *via* a dioxygenation and chloroaniline deamination, resulting in the most likely intermediate product, chlorocatechol [1,13,15]. However, this work is the first to report the possible existence of a second 4CA degradation pathway through aniline. The proposed biodegradation of 4CA in *A. baylyi* GFJ2 is depicted in Fig. 4.

3.6. The biodegradation kinetic and inhibition studies of 34DCA, 4CA and the corresponding intermediates

Because the detection of the transient accumulation of aniline and 4CC established them as intermediates in the 4CA biodegrada-

Table 2
Activities of enzymes involving 4CA and 34DCA biodegradation in cell-free extract of *Acinetobacter baylyi* GFJ2 grown under the condition indicated.

Culture medium and growth substrate[a]	Specific activity (nmole min^{-1} mg protein^{-1})[b]			
	C12DO[c]	CC12DO[c]	C23DO[c]	CC23DO[c]
MMSAY	84 ± 22	9 ± 3	0	0
MMSAY–aniline	437 ± 57	99 ± 24	0	0
MMSAY–catechol	295 ± 50	34 ± 5	0	0
MMSAY–4CC	72 ± 8	406 ± 58	0	0
MMSAY–4CA	306 ± 8	390 ± 21	0	0
MMSAY–34DCA	301 ± 8	272 ± 10	0	0
LB	5 ± 2	0	0	0
LB–aniline	3 ± 1	0	0	0
LB–catechol	5 ± 2	0	0	0
LB–4CC	7 ± 2	5 ± 1	0	0
LB–4CA	6 ± 3	3 ± 1	0	0
LB–34DCA	5 ± 2	3 ± 1	0	0

[a] The culture medium was MMSAY with the supplementation of the indicated substrate at 0.2 mM.
[b] Data were means of the results from four individual experiments and shown with SEs.
[c] C12DO, catechol 1,2-dioxygenase; CC12DO, chlorocatechol 1,2-dioxygenase; C23DO, catechol 2,3-dioxygenase; CC23DO, chlorocatechol 2,3-dioxygenase.

tion pathway, their degradation kinetic parameters (K_s^{app} and k_{max}) were determined. The values of both parameters obtained from non-linear least-squares fitting of the Michaelis–Menten equation and the linear regression of the Lineweaver–Burk plot (data not shown) were in agreement, as shown in Table 1. *A. baylyi* GFJ2 utilized aniline and 4CC at significantly slower rates than 4CA (Table 1). This result explains their accumulation when the 4CA-depletion test was performed at relatively high concentrations (Fig. 3) and suggests that the transformations of aniline and 4CC are probably the limiting steps of 4CA biodegradation.

The biodegradation kinetic study is necessary to provide insights into the mechanism and dynamics of pollutant removal. It also to determine the biodegradation efficiency by providing predictive values for the *in situ* biotransformation mechanism and provide possible limitations for the biodegradation reactions (including substrate and product inhibitions) [27], especially when the intermediates, most of which are structurally related to the toxic chemical of interest, are accumulated. In this case, the influence of 4CA in 34DCA biodegradation and the influences of aniline and 4CC on 4CA biodegradation were evaluated. Generally, the type of inhibition and an inhibition constant are determined using a Dixon plot, in which the reciprocal of the velocity, $1/v$, is plotted against the inhibitor concentration, [I], at two or more substrate concentrations, [S] [9]. However, this plot does not unambiguously distinguished between the competitive and mixed inhibitions [9,28]. Therefore, in this case, the plot of the substrate concentration over the specific reaction velocity, $[S]/v$, was plotted against the inhibitor concentration, [I], to determine the inhibition type (Fig. 5A–C). This plot was subsequently used to determine the apparent dissociation constant of the enzyme–inhibitor (EI) complex (K_i^{app}) and the apparent dissociation constant of the enzyme–substrate–inhibitor (ESI) complex (K_I^{app}) in the mixed inhibition [9] (Fig. 5A and B), while the K_i^{app} of the competitive inhibition was deduced from the Dixon plot (Fig. 5D). This result

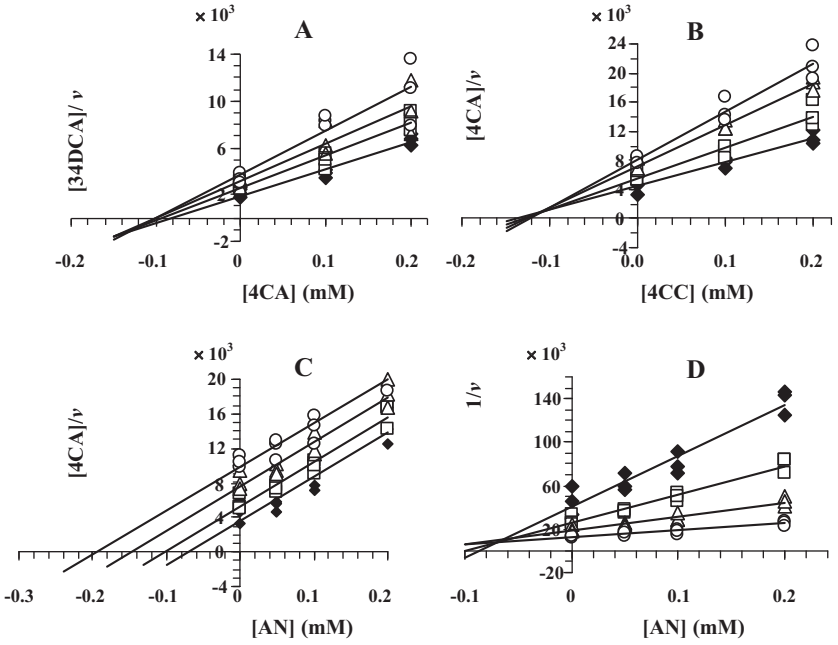

Fig. 5. Characteristic plots for 34DCA and 4CA inhibitions. The plot of the substrate concentration over the specific reaction velocity, $[S]/v$, versus the inhibitor concentration, [I] was used to determined the inhibition type (A–C). The mixed inhibition pattern shown by the influence of 4CA on the degradation of various 34DCA concentrations (mM) (A): 0.05 (♦), 0.1 (□), 0.3(△), 0.5 (○). The uncompetitive inhibition pattern shown by influence of 4CC on the degradation of various 4CA concentrations (mM) (B): 0.1 (♦), 0.2 (□), 0.3(△), 0.5 (○). The competitive inhibition pattern shown by effect of aniline on the degradation of various 4CA concentrations (mM) (C): 0.1 (♦), 0.2 (□), 0.4(△), 0.8 (○). The Dixon plot (D) was used to determine the inhibition coefficient of the competitive inhibition between aniline and 4CA. Data are from at least four individual experiments.

showed that 4CA could act as a strong mixed-competitive inhibitor for 34DCA biodegradation and has the capacity to bind E and ES to form EI and ESI, respectively. This information is not only useful in terms of the understanding of chloroaniline biodegradation mechanism in *A. baylyi* GFJ2, but is also important in designing chloroaniline treatment system, where 4CA and 34DCA generally appear as co-contaminants. As for 4CA degradation in *A. baylyi* GFJ2, 4CC was shown to be an uncompetitive inhibitor (Fig. 5B) that can bind to ES to form an ESI complex. In contrast, aniline acted as a competitive inhibitor (Fig. 5C and D), indicating that it can competitively bind to the same active site of the enzyme responsible for 4CA degradation. Nevertheless, it is premature to conclude that 4CA and aniline are transformed by the same enzyme system. Although there have been several reports on genes involved in aniline biodegradation [29–31], no specific genes for chloroaniline biodegradation have yet been described. Our attempt to obtain genes involved in chloroaniline biodegradation in *A. baylyi* GFJ2 were carried out using probes of the consensus regions described in previous reports, but was unsuccessful. These genes, therefore, remain to be investigated.

4. Conclusions

The *A. baylyi* strain GFJ2 was isolated as a bacterium capable of the efficient biodegradation of 4CA and 34DCA, and broad-range biodegradation of other monohalogenated anilines, including chloro-, bromo-, and fluoro-anilines and DCAs. This work also presents novel, diverse biodegradation pathways for 4CA and 34DCA. While previous reports have demonstrated that 4CA and 34DCA are degraded using separated and unrelated routes, the biodegradation pathways in *A. baylyi* strain GFJ2 are more or less consecutively related. To our knowledge, this is the first report that dechlorination may be involved in 34DCA biodegradation, where 4CA is formed as the first intermediate. However, the mechanism and the enzyme involved in this reaction require further investigation. Furthermore, by detecting the intermediates and characterizing the enzymes involved, this is also the first report that the *A. baylyi* strain GFJ2 has two distinct pathways for 4CA metabolism that yield 4CC or aniline as the first intermediates in each route. The biodegradation results obtained from this study suggest the potential application of *A. baylyi* strain GFJ2 in bioremediation and waste treatment, and the kinetics data also provide insights into the mechanism and dynamics of pollutant removal and the possible limitations of the biodegradation reactions (including substrate and product inhibitions).

Acknowledgements

This work was financially supported by The National Research University Project of CHE and Ratchadaphiseksomphot Endowment Fund (FW 008 B) and the Thai Government Stimulus Package 2 (TKK2555) under the Project for Establishment of Comprehensive Center for Innovative Food, Health Products and Agriculture (PERFECTA).

References

[1] H. Radianingtyas, G.K. Robinson, A.T. Bull, Characterization of a soil-derived bacterial consortium degrading 4-chloroaniline, Microbiology 149 (2003) 3279–3287.
[2] European Chemicals Bureau. 3,4-Dichloroanilines, Summary Risk Assessment Report. Institute for Health and Consumer Protection, Ispra, Italy, 2006.
[3] V.M. Travkin, L.A. Golovleva, The degradation of 3,4-dichloroaniline by *Pseudomonas fluorescens* strain 26-K, Microbiologika 72 (2003) 240–243.
[4] E.G. Surovtseva, V.S. Ivoilov, Y.N. Karasevich, G.K. Vacileva, Chlorinated anilines, a source of carbon, nitrogen and energy for *Pseudomonas diminuta*, Microbiologiya 54 (1985) 948–952.
[5] E.G. Surovtseva, G.K. Vacileva, B.P. Baskunov, A.L. Volnova, Decomposition of 3,4-dichloroaniline by an *Alcaligenes faecalis* culture, Microbiologiia 50 (1981) 740–743.
[6] A.S. Vangnai, W. Petchkroh, Biodegradation of 4-chloroaniline by bacteria enriched from soil, FEMS Microbiol. Lett. 268 (2007) 209–216.
[7] H.J. Stan, Pesticide residue analysis in foodstuffs applying capillary gas chromatography with mass spectrometric detection. State-of-the-art use of modified DFG-multimethod S19 and automated data evaluation, J. Chromatogr. A 892 (2000) 347–377.
[8] S.K. Schmidt, S. Simkins, M. Alexander, Models for the kinetics of biodegradation of organic compounds not supporting growth, Appl. Environ. Microbiol. 50 (1985) 323–331.
[9] A. Cortes, M. Cascante, M.L. Cardenas, A. Cornish-Bowden, Relationships between inhibition constants, inhibitor concentrations for 50% inhibition and types of inhibition: new ways of analysing data, Biochem. J. 357 (2001) 263–268.
[10] V. Helm, H. Reber, Investigation of the regulation of aniline utilization in *Pseudomonas multivorans* strain An1, Eur. J. Appl. Microbiol. Biotechnol. 7 (1979) 191–199.
[11] L.L. Zhang, D. He, J.M. Chen, Y. Liu, Biodegradation of 2-chloroaniline, 3-chloroaniline, and 4-chloroaniline by a novel strain *Delftia tsuruhatensis* H1, J. Hazard. Mater. 179 (2010) 875–882.
[12] B.A. Wiggins, S.H. Jones, M. Alexander, Explanations for the acclimatization period preceding the mineralisation of organic chemicals in aquatic environment, Appl. Environ. Microbiol. 53 (1987) 791–796.
[13] H. Reber, V. Helm, N.G.K. Karanth, Comparative studies on the metabolism of aniline and chloroanilines by *Pseudomonas multivorans* strain An1, Eur. J. Appl. Microbiol. Biotechnol. 7 (1979) 181–189.
[14] A. Farrell, B. Quilty, Substrate-dependent autoaggregation of *Pseudomonas putida* CP1 during the degradation of mono-chlorophenols and phenol, J. Ind. Microbiol. Biotechnol. 28 (2002) 316–324.
[15] J. Zeyer, A. Wasserfallen, K.N. Timmis, Microbial mineralization of ring-substituted anilines through an *ortho*-cleavage pathway, Appl. Environ. Microbiol. 50 (1985) 447–453.
[16] V.M. Travkin, I.P. Solyanikova, I.M. Rietjens, J. Vervoort, W.J. van Berkel, L.A. Golovleva, Degradation of 3,4-dichloro- and 3,4-difluoroaniline by *Pseudomonas fluorescens* 26-K, J. Environ. Sci. Health B 38 (2003) 121–132.
[17] I.S. You, R. Bartha, Metabolism of 3,4-dichloroaniline by *Pseudomonas putida*, J. Agric. Food Chem. 30 (1982) 274–277.
[18] J. Zeyer, P.C. Kearney, Microbial metabolism of propanil and 3,4-dichloroaniline, Pestic. Biochem. Physiol. 17 (1982) 224–231.
[19] D.K. Button, Biochemical basis for whole-cell uptake kinetics: specific affinity, oligotrophic capacity, and the meaning of the Michaelis constant, Appl. Environ. Microbiol. 57 (1991) 2033–2038.
[20] Y. Liu, Overview of some theoretical approaches for derivation of the Monod equation, Appl. Microbiol. Biotechnol. 73 (2007) 1241–1250.
[21] Y. Liu, Y.M. Lin, S.F. Yang, A thermodynamic interpretation of the Monod equation, Curr. Microbiol. 46 (2003) 233–234.
[22] P. Chudoba, B. Capdeville, J. Chudoba, Explanation of biological meaning of the S_0/X_0 ratio in batch cultivation, Water Sci. Technol. 26 (1992) 743–751.
[23] W. Sokol, Oxidation of an inhibitory substrate by washed cells (oxidation of phenol by *Pseudomonas putida*), Biotechnol. Bioeng. 30 (1987) 921–927.
[24] S.C. Chen, K.H. Li, H.Y. Fang, Growth kinetics of EDTA biodegradation by *Burkholderia cepacia*, World J. Microbiol. Biotechnol. 21 (2005) 11–16.
[25] K.H. van Pee, S. Unversucht, Biological dehalogenation and halogenation reactions, Chemosphere 52 (2003) 299–312.
[26] P.M. Kiefer Jr., D.L. McCarthy, S.D. Copley, The reaction catalyzed by tetrachlorohydroquinone dehalogenase does not involve nucleophilic aromatic substitution, Biochemistry 41 (2002) 1308–1314.
[27] A. Monero, L. Lanza, M. Zilli, L. Sene, A. Converti, Batch kinetics of *Pseudomonas* sp. growth on benzene. Modeling of product and substrate inhibitions, Biotechnol. Prog. 19 (2003) 676–679.
[28] M. Schlamowitz, A. Shaw, W.T. Jackson, Limitations of the Dixon plot for ascertaining nature of enzyme inhibition, Tex. Rep. Biol. Med. 27 (1969) 483–488.
[29] E.L. Ang, J.P. Obbard, H. Zhao, Directed evolution of aniline dioxygenase for enhanced bioremediation of aromatic amines, Appl. Microbiol. Biotechnol. 81 (2009) 1063–1070.
[30] L. Geng, M. Chen, Q. Liang, W. Liu, W. Zhang, S. Ping, W. Lu, Y. Yan, W. Wang, M. Takeo, M. Lin, Functional analysis of a putative regulatory gene, *tad*R, involved in aniline degradation in *Delftia tsuruhatensis* AD9, Arch. Microbiol. 191 (2009) 603–614.
[31] Q. Liang, M. Takeo, M. Chen, W. Zhang, Y. Xu, M. Lin, Chromosome-encoded gene cluster for the metabolic pathway that converts aniline to TCA-cycle intermediates in *Delftia tsuruhatensis* AD9, Microbiology 151 (2005) 3435–3446.